Journal of
Materials Chemistry

Cite this: *J. Mater. Chem.*, 2012, **22**, 22913

www.rsc.org/materials

PAPER

Synthesis and photovoltaic performances of conjugated copolymers with 4,7-dithien-5-yl-2,1,3-benzothiadiazole and di(*p*-tolyl)phenylamine side groups†

Haohao Li,[a] Hao Luo,[b] Zhencai Cao,[a] Zhaojie Gu,[a] Ping Shen,[a] Bin Zhao,[a] Huajie Chen,[b] Gui Yu[b] and Songting Tan*[a]

Received 16th June 2012, Accepted 9th September 2012
DOI: 10.1039/c2jm33886f

Three new copolymers (**PT-TPA**, **PT-DTBT** and **PT-DTBTTPA**) based on benzo[1,2-*b*:4,5-*b*] dithiophene (BDT) and thiophene with different conjugated side chains (di(*p*-tolyl)phenylamine (TPA), 4,7-dithien-5-yl-2,1,3-benzothiadiazole (DTBT) and DTBT-TPA) were synthesized *via* Stille coupling polymerization. The TPA and the DTBT were introduced to improve the hole-transport ability and broaden the absorption spectrum. The effects of different conjugated side groups on thermal, optical, electrochemical, hole-transporting and photovoltaic properties of these copolymers were investigated. Field effect results show that the copolymer **PT-DTBTTPA** containing TPA and DTBT in the side chain showed the highest hole mobility. The three copolymers exhibit deep-lying HOMO energy levels, which were effectively tuned by changing the side groups. Photovoltaic cells were fabricated with the synthesized copolymers as electron donors and [6,6]-phenyl-C-butyric acid methyl ester (PCBM) as the electron acceptor. Bulk heterojunction polymer solar cells based on **PT-DTBT** and **PT-DTBTTPA** showed promising power conversion efficiencies of 5.50% and 5.16%, respectively.

Introduction

Bulk heterojunction (BHJ) polymer solar cells (PSCs) based on conjugated copolymers as donors and fullerene derivative as an acceptor[1] have been intensively studied in recent years for their low-cost, lightweight, mechanical flexibility, fast/cheap roll-to-roll production and easy tunability of chemical properties of the photovoltaic materials.[2–5] In the past two years, a lot of new donor–accept (D–A) low band gap polymers have been reported for high-performance PSCs. For example, the solar cells based on the benzo[1,2-*b*:4,5-*b*]dithiophene (BDT) copolymer have achieved a series of high power conversion efficiency (PCE) values in the range 3–8%.[6–9] It is well recognized that to achieve a high efficiency, polymers require a broad absorption spectrum that matches the solar spectrum as well as possible, deep highest occupied molecular orbital (HOMO), and excellent charge transport ability.

For traditional conjugated polymers, it is hard to meet all the above demands. For instance, to broaden the absorption spectrum, we need to increase the length of the conjugated unit of the main chain, which would reduce the hole mobility of the polymer. To pursue the high hole mobility as well as possible, researchers have developed a new family of polymers with conjugated side groups or side chains[10–12] that broaden the absorption spectrum as well as keep the high hole mobility. In our earlier research, we found that the absorption spectrum of a BDT copolymer **PT-DTBTID** containing 1,3-indanedione (ID) and the DTBT side groups has better match with the solar spectrum, but it dramatically decreased the hole mobility and PCE due to the strong electron-withdrawing ability of the ID side group.[12]

Here, we synthesized a new series of conjugated copolymers (**PT-TPA**, **PT-DTBT** and **PT-DTBTTPA**, Fig. 1) by introducing the di(*p*-tolyl)phenylamine (TPA) group with an excellent hole mobility[13] to improve the hole-transport properties of the resulted copolymer. The effects of the conjugated side groups on the thermal, photophysical, electrochemical and photovoltaic properties of the copolymers were investigated in detail, and we acquired the side chain conjugated copolymers with the highest power conversion efficiency reported nowadays.

Experimental section

Material synthesis

4-Methyl-*N*-(4-(4,4,5,5-tetramethyl-1,3,2-dioxaborolan-2-yl) phenyl)-*N*-*p*-tolylbenzenamine (1). A solution of *N*-(4-bromophenyl)-4-methyl-*N*-*p*-tolylbenzenamine (2.11 g, 6 mmol) in 30 mL of anhydrous THF was deoxygenated with nitrogen, and a 2.5 M solution of *n*-butyllithium in hexane (4.8 mL, 12 mmol) was added dropwise at −78 °C. After the solution was stirred at

---

[a] *College of Chemistry, Key Laboratory of Environmentally Friendly Chemistry and Applications of Ministry of Education, Xiangtan University, Xiangtan 411105, P. R. China*
[b] *Beijing National Laboratory for Molecular Science, Institute of Chemistry, Chinese Academy of Sciences, Beijing 100190, P. R. China*

† Electronic supplementary information (ESI) available. See DOI: 10.1039/c2jm33886f

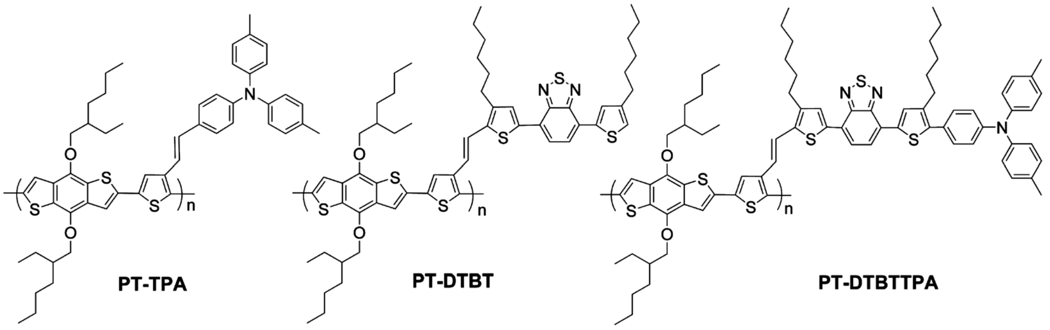

Fig. 1 Molecular structures of **PT-TPA**, **PT-DTBT** and **PT-DTBTTPA**.

−78 °C for 3.5 h, 2-isopropoxy-4,4,5,5-tetramethyl-1,3,2-dioxaborolane (3.96 mL, 18 mmol) was added in one portion. The mixture was stirred at −78 °C for 3 h, and then stirred at room temperature for 36 h. Then, the mixture was poured into water, extracted with diethyl ether and washed with saturated NaCl solution. The organic phase was washed with water and then dried over anhydrous $MgSO_4$. After the solvent was removed by rotary evaporation, the residue was recrystallized. Then, the crude product was filtered and washed with methanol to give a white crystal (1.76 g, 73.5%). ^1H NMR (400 MHz, $CDCl_3$, δ/ppm): 7.64–7.62 (d, 2H, $J = 7.12$ Hz), 7.07–6.97 (m, 10H), 2.33 (s, 6H), 1.34 (s, 12H). MALDI-TOF MS ($C_{26}H_{30}BNO_2$) *m*/*z*: calcd for 399.240, found 399.246.

3-Hexyl-5-(7-(4-hexylthiophene-2-yl)benzo[*c*][1,2,5]thiadiazol-4-yl)thiophene-2-carbaldehyde (3). Compound **3** was synthesized by the Vilsmeier reaction. Under nitrogen atmosphere, to a solution of compound 2 (2.35 g, 5 mmol) in dichloroethane (30 mL), anhydrous DMF (0.4 mL, 5 mmol) was added dropwise, then $POCl_3$ (0.48 mL, 5 mmol) was added slowly at 0 °C. The mixture was stirred at 0 °C for 20 min and then heated to 85 °C for 24 h. After cooling to room temperature, 50 mL water was added to quench the reaction. The mixture was extracted with dichloromethane and washed with water. The organic phase was dried over anhydrous $MgSO_4$ and the solvent was removed by rotary evaporation. The crude product was purified on silica gel chromatography using a petroleum ether–dichloromethane mixture (1/1 by volume) as eluent to afford an orange solid (1.74 g, 70%). FT-IR (KBr, cm^{-1}): 1655 ($\nu_{C=O}$). ^1H NMR (400 MHz, $CDCl_3$, δ/ppm): 10.10 (s, 1H), 8.06–8.04 (d, 2H, $J = 9.28$ Hz), 7.98–7.96 (d, 1H, $J = 7.12$), 7.88–7.86 (d, 1H, $J = 7.28$), 7.10 (s, 1H), 3.05–3.02 (t, 2H, $J = 6.00$ Hz), 2.72–2.69 (t, 2H, $J = 6.00$ Hz), 1.77–1.70 (m, 4H), 1.41–1.34 (m, 12H), 0.90 (m, 6H).

5-(7-(5-Bromo-4-hexylthiophene-2-yl)benzo[*c*][1,2,5]thiadiazol-4-yl)-3-hexylthiophene-2-carbaldehyde (4). Compound **3** (1.74 g, 3.5 mmol) was dissolved in 25 mL of anhydrous DMF. The mixture of *N*-bromosuccinimide (NBS) (0.623 g, 3.5 mmol) and 20 mL anhydrous DMF was added dropwise to the solution and stirred for 24 hours in the dark. Then, the mixture was poured into water and extracted with dichloromethane. The organic phase was dried over anhydrous $MgSO_4$, and then the solvent was removed by rotary evaporation. The crude product was purified on silica gel chromatography using a petroleum ether–dichloromethane mixture (1/1 by volume) as eluent to afford an orange solid (1.71 g, 85%). FT-IR (KBr, cm^{-1}): 1645 ($\nu_{C=O}$). ^1H NMR (400 MHz, $CDCl_3$, δ/ppm): 10.11 (s, 1H), 8.07 (m, 1H), 7.96 (m, 1H), 7.83 (s, 2H), 3.05 (m, 2H), 2.66 (m, 2H), 1.78–1.68 (m, 4H), 1.43–1.35 (m, 12H), 0.92 (m, 6H). MALDI-TOF MS ($C_{27}H_{31}BrN_2OS_3$) *m*/*z*: calcd for 576.080, found 575.987.

5-(7-(5-(4-(Di*p*-tolylamino)phenyl)-4-hexylthiophene-2-yl)benzo[*c*][1,2,5]thiadiazol-4-yl)-3-hexylthiophene-2-carbaldehyde (5). Compound **4** (0.5 g, 0.87 mmol) and compound **1** (0.35 g, 0.87 mmol) were dissolved in 20 mL of anhydrous toluene and deoxygenated with nitrogen for 15 min. $Pd(PPh_3)_4$ (50 mg, 33.75 mmol) was then added under nitrogen and the mixture was again flushed with nitrogen for 30 min. Then the reaction mixture was stirred at 100 °C for 3 days under a nitrogen atmosphere. After cooling to room temperature, the mixture was poured into 50 mL of water and extracted with dichloromethane. The organic phase was washed with water and dried over anhydrous $MgSO_4$. After concentration, the crude product was purified on silica gel chromatography using a petroleum ether–dichloromethane mixture (3/1 by volume) as eluent to afford a purple solid (0.52 g, 77.6%). ^1H NMR (400 MHz, $CDCl_3$, δ/ppm): 10.14 (s, 1H), 8.12–8.10 (d, 2H, $J = 7.16$ Hz), 8.01–8.00 (d, 1H, $J = 7.08$ Hz), 7.91–7.89 (d, 1H, $J = 7.00$ Hz), 7.40–7.38 (d, 2H, $J = 7.36$ Hz), 7.16–7.14 (d, 4H, $J = 7.36$), 7.11–7.10 (d, 6H, $J = 7.12$), 3.10–3.06 (t, 2H, $J = 7.14$ Hz), 2.81–2.78 (m, 2H), 2.38 (s, 6H), 1.84–1.74 (m, 4H), 1.48–1.31 (m, 12H), 0.95–0.94 (m, 6H). ^{13}C NMR (100 MHz, $CDCl_3$, δ/ppm): 182.07, 153.44, 152.48, 147.92, 147.70, 145.00, 141.07, 139.48, 137.28, 135.92, 133.05, 131.38, 130.37, 130.03, 129.71, 128.10, 127.42, 126.86, 125.09, 124.42, 123.83, 121.64, 31.70, 31.50, 31.03, 29.73, 29.28, 29.09, 28.74, 22.66, 20.88, 14.13. MALDI-TOF MS ($C_{47}H_{49}N_3OS_3$) *m*/*z*: calcd for 767.300, found 767.250.

Synthesis of M1. Under a nitrogen atmosphere, 4-di(*p*-tolylamino)benzaldehyde (0.45 g, 1.5 mmol) and compound **6** (0.59 g, 1.5 mmol) were dissolved in 25 mL THF and the solution was stirred at room temperature for 0.5 h. Then the mixture of potassium tertbutoxide (0.15 g, 1.3 mmol) and 15 mL of THF was added dropwise to the solution. The reaction mixture was stirred at room temperature for 5 h, and then heated to 50 °C for 12 h. After cooling to room temperature, the mixture was extracted with dichloromethane and washed with dilute aqueous HCl solution. The organic phase was dried over anhydrous $MgSO_4$, and then the solvent was removed by rotary evaporation. The crude product was purified on silica gel chromatography using a petroleum ether–dichloromethane mixture (4/1 by volume) as eluent to afford a yellow solid (0.39 g, 63.1%). FT-IR (KBr, cm^{-1}): 931 (*trans*-vinylene). ^1H NMR (400 MHz, $CDCl_3$, δ/ppm): 7.13–7.11 (d, 2H, $J = 8.28$ Hz), 7.00 (s, 1H), 6.89–6.87 (d, 4H, $J = 7.84$ Hz), 6.82–6.77 (m, 6H), 6.64 (s, 2H), 2.13 (s, 6H). ^{13}C NMR (100 MHz, $CDCl_3$, δ/ppm): 148.36, 144.92, 139.55, 132.99, 131.06, 129.97, 129.54, 127.41, 124.96, 121.96, 117.79, 111.68, 108.97, 20.85. MALDI-TOF MS ($C_{26}H_{21}Br_2NS$) *m*/*z*: calcd for 539.000, found 539.110.

Synthesis of M3. By following the similar method as for **M1**, **M3** was synthesized from compound 5 (0.4 g, 0.52 mmol) and compound **6** (0.204 g, 0.52 mmol) and potassium tertbutoxide (0.1 g, 0.88 mmol). The crude product was purified on silica gel chromatography using a petroleum ether–dichloromethane mixture (3/1 by volume) as eluent to afford a dark purple solid (0.39 g, 75%). FT-IR (KBr, cm^{-1}): 930 (*trans*-vinylene). ^1H NMR (400 MHz, $CDCl_3$, δ/ppm): 8.15 (s, 1H), 8.08 (s, 1H), 7.98–7.96 (m, 2H), 7.47–7.45 (d, 2H, $J = 8.32$ Hz), 7.32 (s, 2H), 7.23–7.16 (m, 10H), 7.01–6.97 (d, 1H, $J = 16.00$ Hz), 2.88–2.84 (t, 4H, $J = 7.38$ Hz), 2.45 (s, 6H), 1.83–1.82 (m, 4H), 1.48–1.38 (m, 12H), 1.03–1.01 (m, 6H). ^{13}C NMR (100 MHz, $CDCl_3$, δ/ppm): 152.65, 147.76, 145.08, 143.44, 140.08, 139.30, 139.24, 137.55, 136.81, 136.39, 132.95, 130.60, 130.40, 130.01, 129.73, 127.28, 127.16, 126.15, 125.65, 125.03, 124.89, 122.53, 121.78, 119.36, 111.95, 109.74, 31.77, 31.07, 29.32, 29.21, 29.08, 28.71, 22.69, 20.89, 14.16. MALDI-TOF MS ($C_{52}H_{51}Br_2N_3S_4$) *m*/*z*: calcd for 1005.130, found 1005.095.

Synthesis of PT-TPA. To a 50 mL three-neck round bottom flask, **M1** (0.081 g, 0.15 mmol), **M4** (0.115 g, 0.15 mmol) and 15 mL of anhydrous toluene were added. The mixture was deoxygenated with nitrogen for 15 min. $Pd(PPh_3)_4$ (50 mg, 33.75 mmol) was added under nitrogen and the mixture was again flushed with nitrogen for 30 min. Then the reaction mixture was stirred at 100 °C for 3 days under nitrogen atmosphere. After cooling to room temperature, the mixture was slowly poured into methanol (150 mL). The precipitate was collected by filtration and then purified by washing with methanol, hexane and chloroform in a Soxhlet extractor for 24 h in sequence. The dark orange copolymer was recovered from the chloroform fraction by rotary evaporation. Yield: 52 mg (32.5%). FT-IR (KBr, cm^{-1}): 958 (*trans*-vinylene). ^1H NMR (400 MHz, $CDCl_3$, δ/ppm): 7.55–7.37 (br, 3H), 7.07–7.02 (br, 12H), 4.21 (br, 4H), 2.32–2.29 (br, 6H), 1.82–1.26 (br, 20H), 1.00–0.98 (br, 12H). $M_w = 9500$, PDI = 1.57.

Synthesis of PT-DTBTTPA. To a 50 mL three-neck round bottom flask, **M3** (150 mg, 0.15 mmol), **M4** (115 mg, 0.15 mmol) and 15 mL of anhydrous toluene were added. The mixture was deoxygenated with nitrogen for 15 min. $Pd(PPh_3)_4$ (50 mg, 33.75 mmol) was added under nitrogen and the mixture was again flushed with nitrogen for 30 min. Then the reaction mixture was stirred at 100 °C for 3 days under nitrogen atmosphere. After cooling to room temperature, the mixture was slowly poured into methanol (150 mL). The precipitate was collected by filtration and then purified by washing with methanol, hexane and chloroform in a Soxhlet extractor for 24 h in sequence. The purple copolymer was recovered from the chloroform fraction by rotary evaporation. Yield: 114 mg (49.8%). FT-IR (KBr, cm^{-1}): 944 (*trans*-vinylene). ^1H NMR (400 MHz, $CDCl_3$, δ/ppm): 7.81–7.33 (br, 7H), 6.85 (br, 12H), 4.04 (br, 4H), 2.52 (br, 2H), 2.13–1.95 (br, 6H), 1.49–0.65 (br, 56H). $M_w = 15\,000$, PDI = 1.78.

General instrumentation

^1H NMR and ^{13}C NMR spectra were recorded with Bruker AVANCE 400 spectrometer. UV-vis spectra and photoluminescence (PL) spectra of the copolymers were obtained on Perkin-Elmer Lamada 25 spectrometer and Perkin-Elmer LS-50 luminescence spectrometer, respectively. FT-IR spectra were measured on Perkin-Elmer Spectra One. Molecular mass was determined by matrix assisted laser desorption-ionization time-of-flight mass spectrometry (MALDI-TOF MS) using a Bruker Aupoflex-III mass spectrometer. The average molecular weight and polydispersity index (PDI) of the copolymers were determined using Waters 1515 gel permeation chromatography (GPC) analysis with THF as the eluent and polystyrene as the standard. Thermal analyses were performed on a Netzsch TG 209 analyzer and TA DSCQ10 instrument under N_2 atmosphere with a heating and cooling rate of 20 °C min^{-1}. Cyclic voltammetry (CV) was conducted on an electrochemistry workstation (CHI660A, Chenhua Shanghai) with the polymer film on a Pt plate as the working electrode, Pt slice as the counter electrode, and saturated calomel electrode (SCE) as the reference electrode in a 0.1 M tetra-*n*-butylammonium hexafluorophosphate acetonitrile solution at a scan rate of 50 mV s^{-1}.

Fabrication of polymer field-effect transistor devices (FETs)

Polymer-based FETs were fabricated on highly doped silicon wafers with a 300 nm SiO_2 insulator, which was used as gate electrode. The source–drain gold electrodes (30 nm) were prepared by photolithography with the channel length (L) and width (W) of 3 μm and 1400 μm, respectively. The substrates were then subjected to cleaning using ultrasonication in acetone, deionized water, and ethanol. Next, octadecyltrichlorosilane (OTS) treatment was performed on the surface of SiO_2 gate dielectrics in a vacuum to form an OTS self-assembled monolayer. To reduce the contact resistance, the gold drain–source electrodes were modified with pentafluorothiophenol according to the reported methods.[14] Then, a layer of polymer semiconductor film (~40 nm) was deposited on the OTS-modified substrates by spin-coating from a polymer solution in chloroform (10 mg mL^{-1}) at a speed of 2000 rpm for 40 s. For further annealing of the polymer films, the samples were placed on a hotplate at 160 °C in air for 5 minutes before cooling down to room temperature. Field-effect characteristics of the devices were determined in air by using a Keithley 4200 SCS semiconductor parameter analyzer. The field-effect mobility in saturation (μ) is calculated from the equation:

$$I_{DS} = (W/2L)C_i\mu(V_{GS} - V_{th})^2$$

where W/L is the channel width/length, C_i is the insulator capacitance per unit area, and V_{GS} and V_{th} are the gate voltage and threshold voltage, respectively.

Fabrication of photovoltaic devices

The photovoltaic cells were constructed in a traditional sandwich structure. The ITO coated glass substrates were cleaned by successive ultrasonic treatment in acetone and isopropyl alcohol, then treated in a nitrogen–oxygen plasma oven for 5 min. Poly(3,4-ethylene dioxythiophene)-poly(styrenesulfonate) (PEDOT:PSS, from Bayer AG) was spin-coated from an aqueous solution on a cleaned indium tin oxide (ITO) glass substrate giving a thickness of about 40 nm as measured by an Ambios Technology XP-2 surface profilometer. It was then dried at 150 °C for 15 min. Subsequently, the photoactive layer was prepared by spin-coating a dichlorobenzene solution of copolymer : PCBM (1 : 4, w/w), with a polymer concentration of 6 mg mL^{-1}, on the top of the PEDOT:PSS layer giving an active layer thickness of *ca.* 100 nm, and then annealed at 150 °C for 5 min in a nitrogen-filled glovebox. Finally, the substrates were transferred into an evaporator and pumped down to 5×10^{-4} Pa to deposit 5 nm of LiF and 100 nm of aluminum cathode, producing an active area of 4 mm^2 for each cell. Current density–voltage (*J*–*V*) characteristics were measured by a Keithley 2602 Source Meter under 100 mW cm^{-2} irradiation using a 500 W Xe lamp equipped with a global AM 1.5 filter for solar spectrum simulation, and the incident light intensity was calibrated using a standard Si solar cell. The measurement of monochromatic incident photon-to-current conversion efficiency (IPCE) was performed using a Zolix DCS300PA data acquisition system.

Result and discussion

Synthesis and structural characterization

The copolymer structures and synthetic routes are shown in Fig. 1 and Scheme 1. 4,7-Bis-(4-hexylthiophene-2-yl)benzo[1,2,5] thiadiazole (**2**),[15] diethyl-(2,5-dibromothiophene-3-yl)-methylphosphonate (**6**),[16] (*E*)-4-(5-(2-(2,5-dibromothiophene-3-yl) vinyl)-4-hexylthio-phen-2-yl)-7-(4-hexylthiophene-2-yl)benzo [1,2,5]thiadiazole (**M2**) and **PT-DTBT**,[12] and 2,6-bis-(trimethyltin)-4,8-bis(2-ethylhexyloxy)benzo[1,2-*b*:4,5-b′]dithiophene (**M4**),[17] were synthesized according to literature procedures. The aldehyde-functionalized compound **3** was prepared by Vilsmeier–Haack formylation of compound **2** under mild conditions.[18] Bromination of compound **3** with *N*-bromosuccinimide (NBS) yielded compound **4**. A Suzuki coupling reaction was performed between compound **4** and compound **1** to afford compound **5**. The key intermediates, dibromide monomers (**M1**, **M2** and **M3**), were synthesized from compound **6** and aldehyde compounds (4-di(*p*-tolylamino)benzaldehyde, compound **3** and **5**) in moderate yields according to the Witting–Horner reaction. The structures of monomers **M1**, **M2** and **M3** were confirmed by ^{1}H NMR, ^{13}C NMR, FT-IR, and MALDI-TOF MS. The polymerization reaction was proceeded by the Stille coupling polymerization method between **M4** and the monomers **M1**, **M2** and **M3**. All the copolymers exhibited excellent solubility in common organic solvents such as chloroform, tetrahydrofuran, dichloromethane and chlorobenzene. Table 1 summarizes the polymerization results and thermal properties of the copolymers. The molecular weights (M_w) and polydispersity index (PDI) of these copolymers, determined by gel permeation chromatography (GPC) using polystyrenes as standards with tetrahydrofuran as the eluent, were $M_w = 9.5$ kg mol^{-1} with PDI = 1.57 for **PT-TPA**, $M_w = 52.5$ kg mol^{-1} with PDI = 2.6 for **PT-DTBT**, and $M_w = 15.0$ kg mol^{-1} with PDI = 1.78 for **PT-DTBTTPA**.

Thermal properties

The thermal properties of the copolymers were determined by thermogravimetric analysis (TGA) under a nitrogen atmosphere at a heating rate of 20 °C min^{-1}. The three copolymers (**PT-TPA**, **PT-DTBT and PT-DTBTTPA**) have good thermal stability with onset decomposition temperatures (T_d) corresponding to 5% weight loss at 322, 368 and 359 °C, respectively, as shown in Fig. 2 and Table 1. The glass transition temperature of **PT-DTBT** is 155 °C,[12] whereas neither phase transition temperatures nor melting peaks of **PT-TPA** or **PT-DTBTTPA** were observed by differential scanning calorimetry (DSC). Obviously, the thermal stability of these copolymers is adequate for their applications in PSCs and other optoelectronic devices.

Photophysical properties

The photophysical properties of the copolymers are investigated by UV-vis and fluorescence spectroscopy in diluted $CHCl_3$ solution and thin films on quartz plates. Fig. 3 shows the UV-vis absorption spectra and Table 2 summarizes the optical data, including the absorption peak wavelengths ($\lambda_{s,max}$, $\lambda_{f,max}$), absorption edge wavelengths (λ_{edg}) and the optical band gaps. All of the absorption spectra recorded from dilute chloroform solutions feature three absorption bands. The first one around 307 nm results from the *n*–π* transition of TPA group[19] or/and the absorption of the 4,7-dithien-5-yl-2,1,3-benzodiathiazole (DTBT) group. The second absorption band with the absorption maxima ($\lambda_{s,max}$) at 398 nm for **PT-TPA**, 389 nm for **PT-DTBT**, 365 nm for **PT-DTBTTPA** originates from a delocalized excitonic π–π* transition. The third broad band with $\lambda_{s,max}$ at 478, 504 and 497 nm, respectively, corresponds to a localized transition between donor–acceptor charge transfer states, and the intramolecular charge transfer (ICT) between the main chains and the conjugated side chains.[20] Obviously, the localized transition and ICT interactions of the **PT-TPA** progressively decrease due to the disappearance of the DTBT unit and the increase of the electron repellent of the TPA group, the latter reason could also explain the blue-shifted absorption of **PT-DTBTTPA** compared with that of **PT-DTBT**. The absorption spectra of copolymer films are broadened and the peaks are red-shifted compared to their solution absorption spectra, which was mainly attributed to the enhanced intermolecular interactions between neighboring molecules in the film state. The absorption edges of **PT-TPA**, **PT-DTBT** and **PT-DTBTTPA** films are 613, 644 and 673 nm, corresponding to optical band gaps of 2.02, 1.92 and 1.84 eV, respectively.

Fig. 4 shows the photoluminescence (PL) spectra of the copolymers in a dilute chloroform solution. The three copolymers are excited at wavelengths corresponding to the second and third $\lambda_{s,max}$. For instance, **PT-DTBTTPA** exhibits the same PL spectrum when it is excited at 365 and 497 nm, respectively, which indicates that quick and complete intramolecular energy transfer of the excitons occurs from the conjugated side chains to

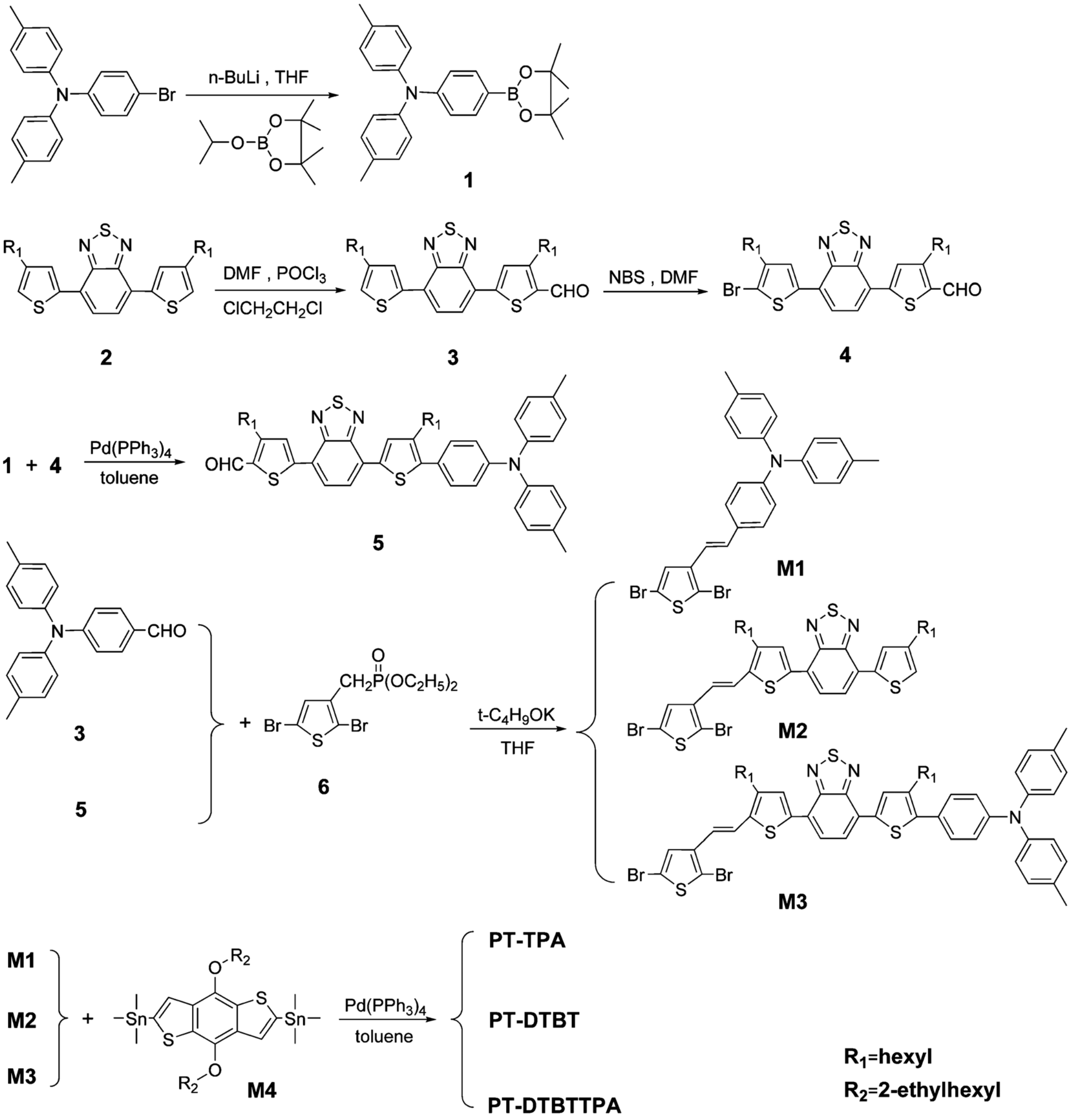

Scheme 1 Synthetic routes of monomers and copolymers.

Table 1 Molecular weights and thermal properties of copolymers

Copolymer	Yield (%)	M_w (Kg mol^{-1})^a	PDI	T_d (°C)^b
PT-TPA	32.5	9.5	1.6	322
PT-DTBT	78.0	52.5	2.6	368
PT-DTBTTPA	49.8	15.0	1.8	359

[a] Determined by GPC in THF, based on polystyrene standards. [b] Decomposition temperature, determined by TGA in nitrogen, based on 5% weight loss.

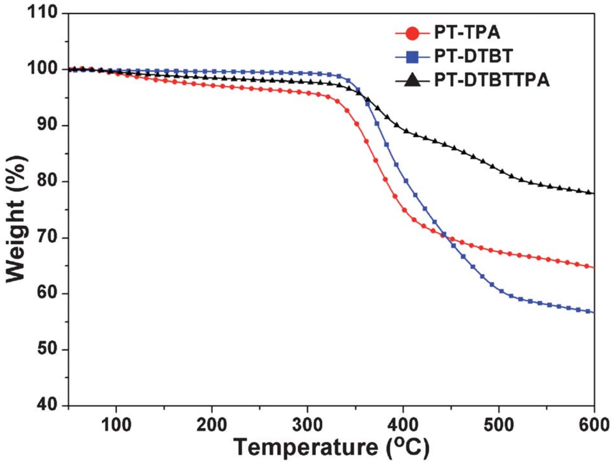

Fig. 2 TGA curves of copolymers at scan rate of 20 °C min^{-1} under nitrogen atmosphere.

the main chains. The phenomenon ensures that the photons absorbed by the polymers are useful for photovoltaic conversion.[21] In $CHCl_3$ solution, **PT-TPA** exhibited a maximum emission peak at 554 nm. With the conjugated DTBT group, **PT-DTBT** and **PT-DTBTTPA** showed similarly red-shifted maximum emission peaks at 682 and 693 nm, respectively,

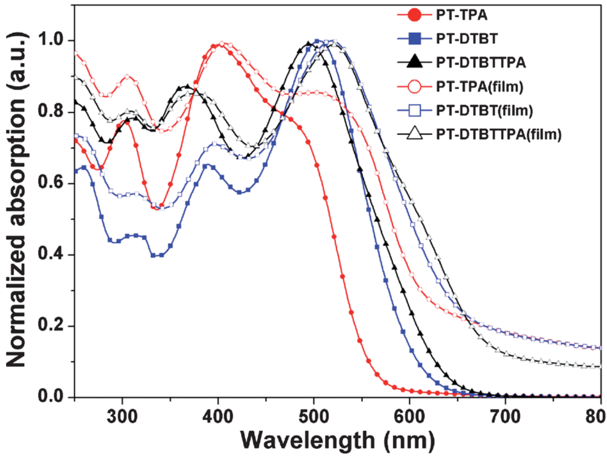

Fig. 3 UV-vis absorption spectra of the copolymers in the $CHCl_3$ solutions and thin films.

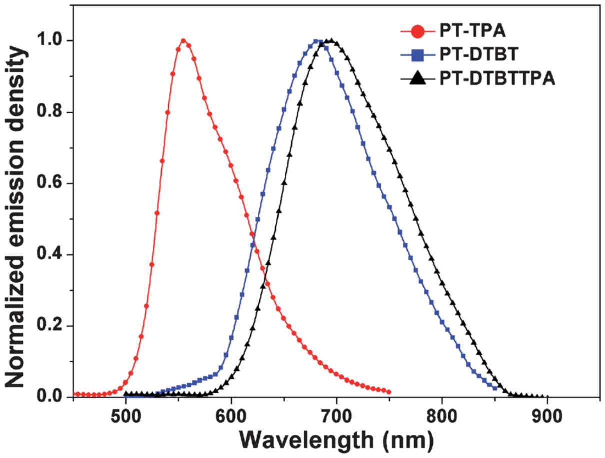

Fig. 4 Photoluminescence spectra of the copolymers in dilute $CHCl_3$.

compared with that of **PT-TPA**. All the results illustrate that the optical properties of the three copolymers can be effectively tuned by changing conjugated side groups.

Electrochemical properties

The electrochemical behavior of the copolymers was investigated by cyclic voltammetry (CV). The cyclic voltammograms of **PT-TPA**, **PT-DTBT** and **PT-DTBTTPA** films are shown in Fig. 5, and Table 2 gives the CV data. The potentials were referenced to the ferrocene/ferrocenium redox couple (Fc/Fc^+). The redox potential of Fc/Fc^+ was assumed to have an absolute energy level of −4.8 eV under vacuum.[22] The redox potential of Fc/Fc^+ was measured under the same conditions as the polymer samples and was located at 0.51 V related to the Saturated Calomel Electrode (SCE). The onset potentials for oxidation (E_{ox}) are observed to be 1.06, 1.15 and 1.09 V for **PT-TPA**, **PT-DTBT** and **PT-DTBTTPA**, respectively. The HOMO energy levels of the copolymers were calculated according to the equation: $HOMO = -e(E_{ox} + 4.29)$ eV. The HOMO energy levels of **PT-TPA**, **PT-DTBT**, and **PT-DTBTTPA** were at −5.35 eV, −5.44 eV, and −5.38 eV respectively. It has been demonstrated that the open-circuit voltage (V_{oc}) value in BHJ solar cells is linearly dependent on the difference between the HOMO level of p-type polymer and the LUMO level of an n-type $PC_{61}BM$.[23] The HOMO energy level of **PT-DTBTTPA** attributed to the introduction of triphenylamine moiety was reduced compared with **PT-DTBT**, indicating that hole-injection and transporting properties have been improved.[24] The copolymer **PT-DTBT** has the lowest HOMO energy level, predicting that it would achieve the highest V_{oc} value. In addition, the deep HOMO levels of the three copolymers are under −5.20 eV, which is the threshold HOMO energy level for air stable conjugated polymers,[25,26] and should be beneficial to their chemical stability in ambient conditions. The LUMO energy levels of **PT-TPA**, **PT-DTBT** and **PT-DTBTTPA** were −3.33, −3.44 and −3.54 eV calculated from the optical band gaps and HOMO energy levels of the copolymers. When comparing the LUMO levels of the polymers and the acceptor (−4.2 eV for $PC_{60}BM$),[27,28] it is seen that the energy differences of LUMO levels are sufficient to result in an efficient charge transfer, that is, higher than the suggested 0.3 eV.[29] Moreover, we found that the LUMO energy levels of the three copolymers **PT-TPA**, **PT-DTBT** and **TP-DTBTTPA** are lowered gradually with the increasing length of the conjugated side chains, which can be attributed to the extension of π-electron delocalization in the copolymer backbone.

Hole mobility

To further understand the effect of the incorporation of the TPA side group and the cause of variation in solar cell performance, the hole mobility of these copolymers was measured using the OTFT technique under the same conditions. **PT-DTBTTPA** with DTBT-TPA side chains demonstrated a higher hole mobility of 4.0×10^{-3} cm^2 V^{-1} s^{-1} than those of **PT-DTBT**

Table 2 Optical and electrochemical properties of the three copolymers

Copolymer	Solution $\lambda_{s,max}$ (nm)[a] Abs.	PL	Film $\lambda_{f,max}$ (nm) Abs.	Film λ_{edge} (nm) Abs.	E_g^{opt} (eV)[b]	HOMO (eV)[c]	LUMO (eV)[d]
PT-TPA	399	554	408	613	2.02	−5.35	−3.33
PT-DTBT	504	682	517	644	1.92	−5.44	−3.44
PT-DTBTTPA	497	693	519	673	1.84	−5.38	−3.54

[a] Measured in chloroform solution. [b] Band gap estimated from the optical absorption band edge of the films. [c] HOMO energy levels measured from cyclic voltammetry. [d] Calculated from the optical band gaps and HOMO energy.

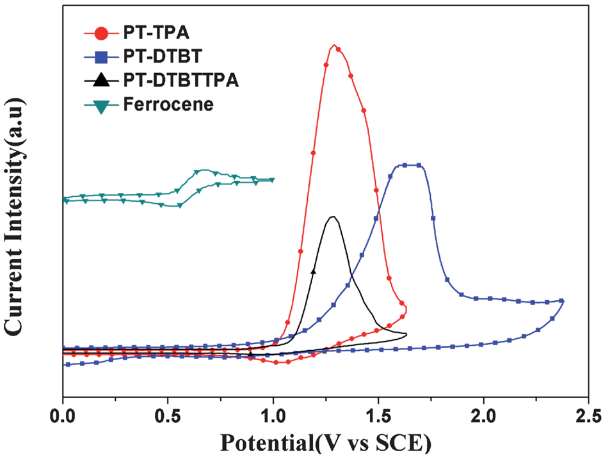

Fig. 5 Cyclic voltammograms of the copolymer films on a platinum electrode in 0.1 mol L^{-1} Bu_4NPF_6 acetonitrile solution. The cyclic voltammogram of ferrocene was also put in the figure for the potential calibration.

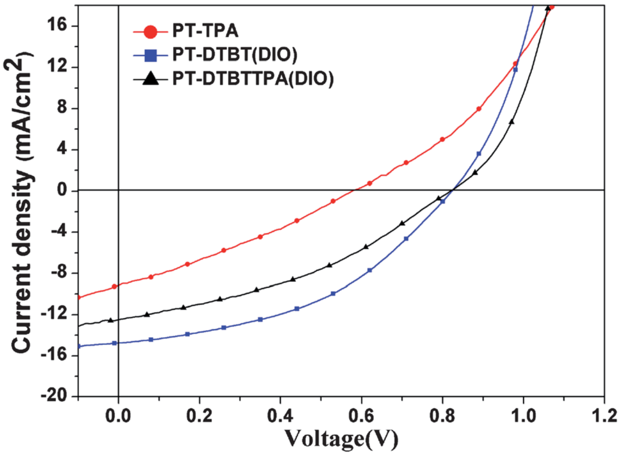

Fig. 6 *J–V* curves of the photovoltaic cells based on **PT-TPA**, **PT-DTBT** and **PT-DTBTTPA** under the illumination of AM 1.5, 100 mW cm^{-2}.

(3.2×10^{-3} cm^2 V^{-1} s^{-1}) and **PT-TPA** (5.5×10^{-4} cm^2 V^{-1} s^{-1}) (Table 3). It is clear that the hole mobility of **PT-DTBTTPA** is higher than that of **PT-DTBT**, which demonstrates that the TPA group actually improved the hole-transporting ability of the copolymer. While the hole mobility of **PT-TPA** is the lowest in the three copolymers, it is still increased visibly compared to that of **PT-ID**.[12] In short, the hole mobility of the three copolymers is relatively high, which is the reason for the high power conversion efficiency.

Photovoltaic properties

In order to check whether the conjugated side groups of the three copolymers make a contribution to the photoelectric conversion in the PSCs, the bulk heterojunction PSCs were fabricated with a device structure of ITO/PEDOT:PSS/polymer : PCBM(1 : 4, w/w)/LiF/Al. The active layers were spin-coated from dichlorobenzene, and in some cases a small amount of the high boiling-point additive 1,8-diiodooctane (DIO) was used to optimize the morphology. Fig. 6 shows the best *J–V* curves of the devices under the illumination of AM 1.5, 100 mW cm^{-2}. The photovoltaic parameters, including the short-circuit current density (J_{sc}), the open-circuit voltage (V_{oc}), the fill factor (FF), and power conversion efficiency (PCE), are summarized in Table 3.

Without the addition of DIO, the power conversion efficiencies for the three copolymers that used $PC_{61}BM$ as the acceptor are in the order of **PT-DTBT** > **PT-DTBTTPA** > **PT-TPA**, and the corresponding data are 4.18%, 3.49%, 1.56%. The sequence of the PCE values for the three copolymers is according to their absorption spectra, V_{oc} values (according to the HOMO energy levels) and the extent of phase separation. Notably, compared with **PT-TPA**, the copolymers **PT-DTBT** and **PT-DTBTTPA**, which contain the DTBT side group, have higher PCE values than that of **PT-TPA**. This is probably due to the strong and broad absorption spectra (Fig. 2). And then compared with **PT-DTBT**, the copolymer **PT-DTBTTPA** exhibits a slightly lower PCE value although the addition of the TPA group on the side chain enhances the hole mobility. That is because the J_{sc} value of **PT-DTBT** is higher than that of **PT-DTBTTPA** due to the different phase separation state. From the atomic force microscopy (AFM) images of three copolymers (Fig. 7) and the amplified AFM phase images (Fig. S13†) of **PT-DTBTTPA**-$PC_{61}BM$ with and without DIO, we can see that there is no large phase separation for **PT-DTBT**, but the phase separation for **PT-TPA** and **PT-DTBTTPA** are relatively obvious. However, it is clear that the phase separation for **PT-DTBTTPA** has been improved obviously by adding 1% DIO. As we know, the use of high-boiling-point additives such as DIO could promote the packing of the polymer by avoiding excessive crystallization of

Table 3 Photovoltaic properties and mobility of the copolymers and PCBM (1 : 4, w/w)

Copolymer	PCBM(DIO)	Thickness (nm)	J_{sc} (mA cm^{-2})	V_{oc} (V)	FF	$PCE_{max}(PCE_{ave})$ (%)	$\mu_{h,ave}(\mu_{h,max})$ (cm^2 V^{-1} s^{-1})
PT-TPA	$PC_{61}BM$(–)	120	9.17	0.58	0.32	1.56(1.32)	$5.5 \times 10^{-4}(6.0 \times 10^{-4})$
PT-DTBT	$PC_{61}BM$(–)	110	12.65	0.81	0.41	4.18(4.07)	$3.2 \times 10^{-3}(8.0 \times 10^{-3})$
	$PC_{61}BM$(1%)	100	14.88	0.83	0.43	5.35(5.21)	
	$PC_{61}BM$(2%)	110	13.58	0.81	0.39	4.24(4.18)	
	$PC_{61}BM$(3%)	110	11.54	0.76	0.36	3.18(3.04)	
	$PC_{71}BM$(1%)	100	14.64	0.79	0.48	5.50(5.30)	
PT-DTBTTPA	$PC_{61}BM$(–)	110	9.49	0.78	0.47	3.49(3.27)	$4.0 \times 10^{-3}(4.5 \times 10^{-3})$
	$PC_{61}BM$(1%)	100	12.47	0.82	0.37	3.81(3.66)	
	$PC_{71}BM$(1%)	100	14.26	0.77	0.47	5.16(5.01)	

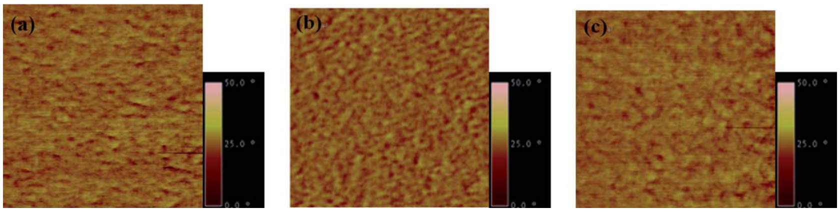

Fig. 7 AFM phase images (500 × 500 nm) for copolymer : $PC_{61}BM$ blend films: (a) **PT-TPA**, (b) **PT-DTBT** and (c) **PT-DTBTTPA**.

the fullerene,[30] which is beneficial to improve the PCE of the copolymers. Therefore, the devices of **PT-DTBT** with different DIO ratios were studied, and a ratio of 1% showed the best device performance of 5.35%. Then we measured a **PT-DTBTTPA**-based device using this ratio of DIO. As a result, the PCE of **PT-DTBTTPA** improved slightly from 3.48% to 3.81%, compared to that of **PT-DTBT**, which was improved from 4.18% to 5.35%.

In addition, the photovoltaic properties of **PT-DTBT** and **PT-DTBTTPA** were investigated in BHJ solar cells using $PC_{71}BM$ as the acceptor. We obtain the maximum power conversion efficiency of 5.50% based on **PT-DTBT** ($J_{sc} = 14.64$ mA cm^{-2}, $V_{oc} = 0.79$ V, FF = 0.48). It is noteworthy that the PCE of **PT-DTBTTPA** cannot exceed the PCE of **PT-DTBT**, but the PCE of **PT-DTBTTPA** improved significantly from 3.81% to 5.16%. It can account for the obvious increase in J_{sc} as revealed by incident-photon-to-current efficiency (IPCE) spectra (Fig. 8), which may result from the better charge transfer and the decrease of electron aggregation by improving the miscibility between **PT-DTBTTPA** and $PC_{71}BM$. According to the data, it is clear that the efficiencies of the PSCs can be strongly affected by TPA and DTBT side groups in the backbone of copolymer molecules.

Conclusion

In summary, three novel benzo[1,2-*b*:4,5-*b*]dithiophene and thiophene copolymers with TPA, DTBT and DTBT-TPA side groups are successfully synthesized and characterized. All of the copolymers are found to exhibit good thermal stability. The research results show that the conjugated side groups can broaden the absorption spectrum as well as improve the hole-transporting properties of copolymers, and as a result, improve the power conversion efficiencies. These copolymers appear promising for application in BHJ solar cells due to their good solubilities and their low band gaps as well as their high hole mobilities. The broad absorption spectra, deep HOMO levels and the noticeably high hole mobilities of **PT-DTBT** and **PT-DTBTTPA** contribute to the outstanding J_{sc}, V_{oc} as well as the high device efficiencies over 5.0%. The best PCE of the device based on **PT-DTBT** reached 5.50%, which shows that **PT-DTBT** is promising for the potential application of photovoltaic cells.

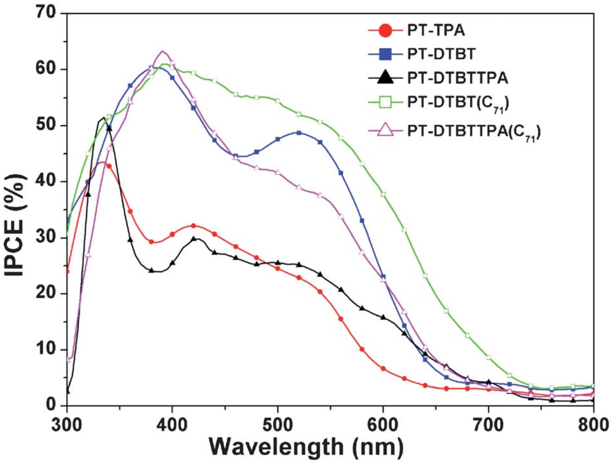

Fig. 8 IPCE of the copolymer solar cells based on **PT-TPA**, **PT-DTBT** and **PT-DTBTTPA**.

Acknowledgements

This work was supported by the National Nature Science Foundation of China (50973092, 51003089, 21004050, 51173154), National Basic Research Program of China (2011CBA00701), and Specialized Research Fund for the Doctoral Program of Higher Education of China (20094301120005, 20104301110003), and Open Fund of Key Laboratory of Advanced Functional Polymeric Materials of College of Hunan Province (09K037).

References

1 F. Huang, K. S. Chen, H. L. Yip, S. K. Hau, O. Acton, Y. Zhang, J. D. Luo and A. K. Y. Jen, *J. Am. Chem. Soc.*, 2009, **131**, 13886.
2 G. Yu, J. Gao, J. C. Hummelen, F. Wudl and A. J. Heeger, *Science*, 1995, **270**, 1789.
3 J. Chen and Y. Cao, *Acc. Chem. Res.*, 2009, **42**, 1709.
4 (*a*) Y. F. Li and Y. P. Zou, *Adv. Mater.*, 2008, **20**, 2952; (*b*) Y. F. Li, *Acc. Chem. Res.*, 2012, **45**, 723.
5 (*a*) T. Y. Chu, J. Lu, S. Beaupre, Y. Zhang, J. R. Pouliot, S. Wakim, J. Zhou, M. Leclerc, Z. Li, J. Ding and Y. Tao, *J. Am. Chem. Soc.*, 2011, **133**, 4250; (*b*) P. Sista, M. C. Biewer and M. C. Stefen, *Macromol. Rapid Commun.*, 2012, **33**, 9.
6 (*a*) Y. Liang, D. Feng, Y. Wu, S. T. Tsai, G. Li, C. Ray and L. Yu, *J. Am. Chem. Soc.*, 2009, **131**, 7792; (*b*) L. J. Huo, J. H. Hou, S. Q. Zhang, H. Y. Chen and Y. Yang, *Angew. Chem.*, 2010, **122**, 1542; (*c*) R. M. Duan, L. Ye, X. Guo, Y. Huang, P. Wang, S. Q. Zhang, J. P. Zhang, L. J. Huo and J. H. Hou, *Macromolecules*, 2012, **45**, 3032.
7 (*a*) M. Wang, X. W. Hu, P. Liu, W. Li, X. Gong, F. Huang and Y. Cao, *J. Am. Chem. Soc.*, 2011, **133**, 9638; (*b*) L. J. Huo, S. Q. Zhang, X. Guo, F. Xu, Y. F. Li and J. H. Hou, *Angew. Chem., Int. Ed.*, 2011, **50**, 9697; (*c*) Y. Huang, X. Guo, F. Liu, L. J. Huo, Y. N. Chen, T. P. Russell, C. C. Han, Y. F. Li and J. H. Hou, *Adv. Mater.*, 2012, **24**, 3383.
8 (*a*) C. Piliego, T. W. Holcombe, J. D. Douglas, C. H. Woo, P. M. Beaujuge and J. M. J. Fréchet, *J. Am. Chem. Soc.*, 2010, **132**, 7595; (*b*) J. D. Douglas, G. Griffini, T. W. Holcombe, E. P. Young, O. P. Lee, M. S. Chen and J. M. J. Frechet, *Macromolecules*, 2012, **45**, 4069.
9 J. M. Cao, W. Zhang, Z. Xiao, L. Y. Liao, W. G. Zhu, Q. Q. Zuo and L. M. Ding, *Macromolecules*, 2012, **45**, 1710.

10 (*a*) J. H. Hou, Z. A. Tan, Y. Yan, Y. J. He, C. H. Yang and Y. F. Li, *J. Am. Chem. Soc.*, 2006, **128**, 4911; (*b*) X. C. Wang, Y. P. Sun, S. Chen, X. Guo, M. J. Zhang, X. Y. Li, Y. F Li and H. Q. Wang, *Macromolecules*, 2012, **45**, 1208; (*c*) Z. G. Zhang, S. Y. Zhang, J. Min, C. H. Cui, H. Geng, Z. G. Shuai and Y. F. Li, *Macromolecules*, 2012, **45**, 2312.

11 Z. J. Gu, P. Shen, S. W. Tsang, Y. Tao, B. Zhao, P. Tang, Y. J. Nie, Y. Fang and S. T. Tan, *Chem. Commun.*, 2011, **47**, 9381.

12 Z. J. Gu, P. Tang, B. Zhao, H. Luo, X. Guo, H. J. Chen, G. Yu, X. P. Liu, P. Shen and S. T. Tan, *Macromolecules*, 2012, **45**, 2359.

13 P. Cias, C. Slugovc and G. Gescheidt, *J. Phys. Chem. A*, 2011, **115**, 14519.

14 Y. Zhao, C. A. Di, X. K. Gao, Y. B. Hu, Y. L. Guo, L. Zhang, Y. Q. Liu, J. Z. Wang, W. P. Hu and D. B. Zhu, *Adv. Mater.*, 2011, **23**, 2448.

15 S. Zhang, Y. Guo, H. Fan, Y. Liu, H. Chen, G. Yang, X. Zhan, Y. Liu, Y. Li and Y. Yang, *J. Polym. Sci., Part A: Polym. Chem.*, 2009, **47**, 5498.

16 J. H. Hou, L. Huo, C. He, C. Yang and Y. F. Li, *Macromolecules*, 2006, **39**, 594.

17 Y. J. Nie, B. Zhao, P. Tang, P. Jiang, Z. F. Tian, P. Shen and S. T. Tan, *J. Polym. Sci., Part A: Polym. Chem.*, 2011, **49**, 3604.

18 P. Shen, Y. J. Liu, X. W. Huang, B. Zhao, N. Xiang, J. J. Fei, L. M. Liu, X. Y. Wang, H. Huang and S. T. Tan, *Dyes Pigm.*, 2009, **83**, 187.

19 (*a*) Z. G. Zhang, K. L. Zhang, G. Liu, C. X. Zhu, K. G. Neoh and E. T. Kang, *Macromolecules*, 2009, **42**, 3104; (*b*) Z. G. Zhang, Y. L. Liu, Y. Yang, K. Hou, B. Peng, G. Zhao, M. Zhang, X. Guo, E. T. Kang and Y. Li, *Macromolecules*, 2010, **43**, 9376.

20 J. K. Jin, J. K. Choi, B. J. Kim, H. B. Kang, S. C. Yoon, H. You and H. T. Jung, *Macromolecules*, 2011, **44**, 502.

21 P. Shen, T. P. Ding, H. Huang, B. Zhao and S. T. Tan, *Synth. Met.*, 2010, **160**, 1291.

22 Y. Li, Y. Cao, J. Gao, D. Wang, G. Yu and A. J. Heeger, *Synth. Met.*, 1999, **99**, 243.

23 Y. J. Cheng, S. H. Yang and C. S. Hsu, *Chem. Rev.*, 2009, **109**, 5868.

24 P. Shen, G. Y. Sang, J. J. Lu, B. Zhao, M. X. Wan and Y. P. Zou, *et al.*, *Macromolecules*, 2008, **41**, 5716.

25 B. C. Thompson, Y. G. Kim and J. R. Reynolds, *Macromolecules*, 2005, **38**, 5359.

26 D. M. D. Leeuw, M. M. J. Simenon, A. R. Brown and R. E. F. Einerhand, *Synth. Met.*, 1997, **87**, 53.

27 A. Varotto, N. D. Treat, J. Jo, C. G. Shuttle, N. A. Batara, F. G. Brunetti, J. H. Seo, M. L. Chabinyc, C. J. Hawker, A. J. Heeger and F. Wudl, *Angew. Chem., Int. Ed.*, 2011, **50**, 5166.

28 Y. M. Sun, G. C. Welch, W. L. Leong, C. J. Takacs, G. C. Bazan and A. J. Heeger, *Nat. Mater.*, 2012, **11**, 44.

29 J. L. Brédas, D. Beljonne, V. Coropceanu and J. Cornil, *Chem. Rev.*, 2004, **104**, 4971.

30 J. Peet, N. S. Cho, S. K. Lee and G. C. Bazan, *Macromolecules*, 2008, **41**, 8655.